



Published in final edited form as:

Nature. 2013 April 4; 496(7443): 114–118. doi:10.1038/nature11998.

## Mechanistic studies of an unprecedented enzyme-catalyzed 1,2-phosphono migration reaction

Wei-chen Chang<sup>1,‡</sup>, Mishtu Dey<sup>2,†,‡</sup>, Pinghua Liu<sup>1,†,‡</sup>, Steven O. Mansoorabadi<sup>1,†,‡</sup>, Sung-Ju Moon<sup>1,†,‡</sup>, Zongbao K. Zhao<sup>1,‡</sup>, Catherine L. Drennan<sup>2</sup>, and Hung-wen Liu<sup>1,\*</sup>

<sup>1</sup>Division of Medicinal Chemistry, College of Pharmacy, and Department of Chemistry and Biochemistry, University of Texas at Austin, Austin, TX 78712, USA

<sup>2</sup>Howard Hughes Medical Institute and the Departments of Chemistry and Biology, Massachusetts Institute of Technology, Cambridge, MA 01239, USA

### Abstract

(*S*)-2-Hydroxypropylphosphonate ((*S*)-2-HPP) epoxidase (HppE) is a mononuclear non-heme iron-dependent enzyme<sup>1,2,3</sup> responsible for the last step in the biosynthesis of the clinically useful antibiotic fosfomycin<sup>4</sup>. Enzymes of this class typically catalyze oxygenation reactions that proceed via the formation of substrate radical intermediates. In contrast, HppE catalyzes an unusual dehydrogenation reaction while converting the secondary alcohol of (*S*)-2-HPP to the epoxide ring of fosfomycin<sup>1,5</sup>. HppE is shown here to also catalyze a biologically unprecedented 1,2-phosphono migration with the alternative substrate (*R*)-1-HPP. This transformation likely involves an intermediary carbocation based on observations with additional substrate analogues, such as (*1R*)-1-hydroxy-2-aminopropylphosphonate, and model reactions for both radical- and carbocation-mediated migration. The ability of HppE to catalyze distinct reactions depending on the regio- and stereochemical properties of the substrate is given a structural basis using X-ray crystallography. These results provide compelling evidence for the formation of a substrate-derived cation intermediate in the catalytic cycle of a mononuclear non-heme iron-dependent enzyme. The underlying chemistry of this unusual phosphono migration may represent a new paradigm for the *in vivo* construction of phosphonate-containing natural products that can be exploited for the preparation of novel phosphonate derivatives.

Users may view, print, copy, download and text and data- mine the content in such documents, for the purposes of academic research, subject always to the full Conditions of use: [http://www.nature.com/authors/editorial\\_policies/license.html#terms](http://www.nature.com/authors/editorial_policies/license.html#terms)

\*Correspondence and requests for material should be addressed to H.-w. L. (h.w.liu@austin.utexas.edu).

†These authors contributed equally to the work described in this manuscript.

‡Current address: W.-c.C., Department of Chemistry, Penn State University, University Park, PA 16802, USA; M.D., Department of Chemistry, University of Iowa, Iowa City, IA 52242, USA; P.L., Department of Chemistry, Boston University, Boston, MA 02215, USA; S.O.M., Department of Chemistry and Biochemistry, Auburn University, Auburn, AL 36849, USA; S.-J.M., Agensys Inc., Santa Monica, CA 90404, USA; Z.K.Z., Department of Biotechnology, Dalian Institute of Chemical Physics, Dalian 116023, PR China.

Supplementary Information and the associated references are available in the online version of the paper at [www.nature.com/nature](http://www.nature.com/nature).

**Author Contributions:** H.-w.L. provided the scientific direction and overall experimental design for the studies. W.-c.C. performed many of the experiments describe herein. M.D. and C.D. collected and interpreted all of the crystallographic data. P.L., S.-J.M. and Z.K.Z. designed and carried out the initial biochemical as well as model system studies. S.O.M. performed the DFT calculations. W.-c.C., M.D., P.L., S.O.M., C.D., and H.-w.L. wrote the manuscript.

**Author Information:** Atomic coordinates and structure factors have been deposited in the Protein Data Bank (PDB) under accession codes 4J1W and 4J1X. Reprints and permissions information is available at [www.nature.com/reprints](http://www.nature.com/reprints). The authors declare no competing financial interests. Readers are welcome to comment on the online version of this article at [www.nature.com/nature](http://www.nature.com/nature).

Fosfomycin (**1**) is a clinically useful antibiotic for the treatment of limb-threatening diabetic foot infections and lower urinary tract infections<sup>4</sup>. Its biological target is UDP-GlcNAc-3-*O*-enolpyruvyltransferase (MurA), which catalyzes the first committed step in the biosynthesis of peptidoglycan, the main component of the bacterial cell wall<sup>6, 7</sup>. Importantly, fosfomycin has been shown to be effective against ciprofloxacin-resistant *Escherichia coli*<sup>8</sup>, and methicillin- or vancomycin-resistant strains of *Staphylococcus aureus*<sup>9, 10</sup>. Fosfomycin is derived from phosphoenolpyruvate (PEP, **2**), with the phosphonate moiety being generated in a rearrangement reaction catalyzed by PEP mutase (**2**→**3**, Fig. 1A)<sup>11, 12</sup>. This is followed by a reaction sequence involving decarboxylation, reduction, and C-methylation to produce (*S*)-2-hydroxypropylphosphonate ((*S*)-2-HPP, **4**)<sup>13, 14</sup>. The final step of the pathway is the conversion of (*S*)-2-HPP (**4**) to fosfomycin (**1**) catalyzed by (*S*)-2-HPP epoxidase (HppE)<sup>1, 2</sup>.

Early studies showed that HppE is a mononuclear non-heme iron-dependent enzyme<sup>1, 2</sup> that employs a 2-His-1-carboxylate facial triad as the iron ligands and its overall structural fold belongs to the cupin superfamily<sup>3, 15</sup>. However, unlike many other enzymes in this class<sup>16</sup>, its activity is not dependent on  $\alpha$ -ketoglutarate. Instead, HppE utilizes reducing equivalents derived from NADH to activate molecular oxygen<sup>1, 2</sup>. Furthermore, isotope-labeling experiments demonstrated that the oxygen atom of the oxiranyl ring in **1** is not derived from O<sub>2</sub>, but instead from the secondary hydroxyl group of **4** (Fig. 1A)<sup>1, 5</sup>. Thus, the HppE-catalyzed conversion of **4** to **1** is in fact a dehydrogenation reaction and not an oxygenation reaction.

Previous experiments have also shown that the HppE reaction course is dependent on the substrate stereochemistry, since the HppE-catalyzed dehydrogenation of (*R*)-2-HPP (**5**) produces the ketone **6** rather than an epoxide (Fig. 1B)<sup>17</sup>. Recent spectroscopic and crystallographic studies revealed that both enantiomers of 2-HPP (**4** and **5**) act as bidentate ligands to the mononuclear iron, such that only a single hydrogen atom is poised for abstraction by a reactive iron-oxygen species<sup>3, 18, 19</sup>. The direct coordination of the negatively charged phosphonate group to the iron center likely helps to activate Fe<sup>II</sup> for reaction with O<sub>2</sub> and thus facilitates the formation of higher iron oxidation states for substrate oxidation<sup>3, 20, 21</sup>. These findings prompted a more thorough examination of the substrate flexibility and reactivity of HppE. Toward this aim, both enantiomers of 1-hydroxypropylphosphonate (**7**, 1-HPP) were synthesized and used as mechanistic probes of the HppE-catalyzed reaction<sup>22</sup>.

Incubation of (*S*)-**7** with HppE produced the acyl phosphonate **8** (Fig. 1C and Fig. 2A), a reaction analogous to the dehydrogenation of (*R*)-2-HPP (**5**) to form the corresponding C2 ketone (**6**, Fig. 1B). Both reactions are consistent with H-atom abstraction from the oxygen bearing carbon to yield an  $\alpha$ -hydroxyalkyl radical that undergoes one electron oxidation to form the corresponding oxo product. In contrast, when (*R*)-**7** was treated with HppE, 1-oxopropan-2-ylphosphonate (**9**) was obtained as the sole product (Fig. 1D and Fig. 2B). The structure of **9** was initially determined by NMR, and was verified after NaBH<sub>4</sub> reduction to the more stable product 1-(hydroxymethyl)ethylphosphonate (**10**) and comparison with the chemically synthesized standard<sup>23</sup>. To further validate the structure of **9**, (*R*)-**7** was prepared enriched with <sup>13</sup>C at C1 ((*R*)-[1-<sup>13</sup>C]-**7**) and used as the substrate in the HppE reaction<sup>22</sup>.

Analysis by  $^{13}\text{C}$  NMR demonstrated that the large C1-P coupling constant of 150.0 Hz in (*R*)-[1- $^{13}\text{C}$ ]-**7** was reduced to 2.7 Hz in **10** following reaction with HppE. These results indicate that HppE catalyzes a 1,2-shift of the phosphono group during catalytic turnover of the substrate analogue (*R*)-**7**, for which there is no enzymatic precedent.

The crystal structures of  $\text{Fe}^{\text{II}}$ -HppE in complex with (*R*)-**7** and (*S*)-**7** were determined to 2.71 and 2.80 Å resolution, respectively, in order to provide a structural basis for the altered stereo- and regioselectivity of the HppE-catalyzed reactions with these substrates<sup>22</sup>. Our results showed that (*R*)- and (*S*)-**7** bind to the iron center in a bidentate fashion via an oxygen from the phosphonate moiety and the C1 hydroxyl (Fig. 3, Supplementary Fig. 5-6). Three additional coordination sites of the iron are filled by the 2-His-1-carboxylate facial triad, leaving one site available for dioxygen binding. This site, partially occupied by a water molecule in these structures, is the same putative  $\text{O}_2$ -binding pocket to which the  $\text{O}_2$ -mimic nitric oxide binds<sup>18</sup>. This spatial arrangement would direct the C1 hydrogen of (*S*)-**7** and the *pro-R* C2 hydrogen of (*R*)-**7** towards the reactive iron-oxygen species, consistent with the observed reaction products **8** and **9**.

To verify the stereochemistry of hydrogen atom abstraction from the prochiral carbon of (*R*)-**7**, substrate stereospecifically deuterated at the *pro-R* (**11**) or *pro-S* (**12**) positions of C2 were synthesized (Supplementary Fig. 2) and reacted with HppE.  $^1\text{H}$  NMR analysis of the methyl group splitting pattern of the reaction products from both diastereomers (Supplementary Fig. 3) demonstrated retention of only the *pro-S* hydrogen, consistent with the stereospecific abstraction of the *pro-R* hydrogen atom from C2 of (*R*)-**7** (Fig. 4A)<sup>22</sup> predicted by crystal structural analysis (Fig. 3).

While non-enzymatic 1,2-phosphono migrations are known, they require either strong Lewis acids<sup>24</sup> or harsh alkaline conditions<sup>25</sup> and are generally thought to proceed through carbocationic intermediates. It is therefore plausible that such an intermediate may also be involved in the HppE-catalyzed 1,2-phosphono migration of (*R*)-**7** (Fig. 4B, route a). Following *pro-R* hydrogen atom abstraction by a reactive iron-oxygen species to form the C2-centered radical **14**, electron transfer to the iron center would produce the corresponding C2 carbocation **15**. This oxidation would then trigger the 1,2-phosphono migration in direct analogy to the non-enzymatic reactions. However, an alternative route involving a C2 radical-mediated migration of the C-P bond to generate the ketyl radical **16** prior to electron transfer could not be excluded (Fig. 4B, route b).

To gain insight into the chemistry of the defining intermediates of these two mechanistic hypotheses, model studies were carried out with compounds **17** and **18**<sup>22</sup>. As summarized in Figure 4C, when **17** was treated with silver triflate to generate the carbocation intermediate **19**, the migration product **20** was produced. In contrast, when the alkyl radical **21** was generated, either by exposure of compound **18** to UV radiation or treatment of **17** with tributyltin hydride, formation of alkene **22** was observed. These findings provide a correlation between formation of a carbocation intermediate and 1,2-phosphono migration. It is also worth noting that the intermediacy of carbocationic species has been implicated in most biological 1,2-hydride and 1,2-alkyl shift reactions, such as those catalyzed by various terpenoid cyclases<sup>26</sup> and the “NIH shift” of aromatic amino acid hydroxylases<sup>27</sup>. However,

the situation could still be different on the enzyme since, in the model reaction, formation of **22** from **21** may simply be more rapid than rearrangement to form **20** in solution.

Further evidence supporting a carbocationic intermediate in the HppE-catalyzed reaction was obtained using the substrate analogues (1*R*,2*R*)- and (1*R*,2*S*)-1-hydroxyl-2-aminopropyl-phosphonate ((*RR*)- and (*RS*)-**23**, Fig. 4D)<sup>22</sup>. Using a NMR assay and authentic standards (Supplementary Fig. 4)<sup>22</sup>, HppE was shown to convert both isomers of **23** to **26** with no detectable formation of the migration or other product. This ketone product can be envisioned as forming via hydrogen atom abstraction from C2, yielding an  $\alpha$ -aminoalkyl radical (**24**) that is oxidized to the stable C2 iminium ion **25**, which can undergo spontaneous hydrolysis to yield **26**. Hydrogen atom abstraction from C2 and the conversion of both isomers of **23** to **26** are consistent with bidentate coordination to the active site iron through the C1 hydroxyl and phosphonate moieties, in a manner analogous to (*R*)-**7** (Supplementary Fig. 7, 8). Support for the hypothesis that the C2 amino group of **23** is unable to sustain the bidentate substrate coordination required for catalysis was obtained with the substrate analogue 2-aminopropylphosphonate (( $\pm$ )-**27**, Fig. 4D), which lacks the 1-hydroxyl group of **23** and is not a substrate of HppE<sup>22</sup>. Taken together, these results are consistent with a mechanism in which a reactive iron-oxygen species generated during the catalytic cycle of HppE is capable of oxidizing the C2-centered radical **24** to the corresponding carbocation **25** during the conversion of **23** to **26** (Fig. 4D).

In summary, this investigation provides new insight into the catalytic capability and chemical mechanism of the non-heme iron enzyme HppE. HppE displays remarkable catalytic versatility, converting the (*R*)- and (*S*)-isomers of 1- and 2-HPP to aldehyde, acyl phosphonate, ketone, and epoxide products, respectively (Fig. 1). This study reveals an unprecedented 1,2-phosphono migration reaction and provides support for the existence of carbocation intermediates in the HppE reaction. The unique chemistry observed during the phosphono migration reaction catalyzed by HppE may represent a new paradigm for the rearrangement of C-P bonds in Nature, which can be exploited for the synthesis of novel phosphonate-containing natural products. Moreover, the likely use of a carbocation intermediate in the HppE-catalyzed conversion of **23** to **26**, buoys the proposal of a carbocation (**15**) intermediate in the conversion of (*R*)-**7** to **9** (phosphono migration product in Fig. 1D), and prompts reexamination of the mechanism of HppE in general. In terms of the types of iron-oxygen species employed by HppE, <sup>18</sup>O kinetic isotope effect (KIE) studies with the natural substrate, (*S*)-2-HPP (**4**), demonstrate partially rate-limiting formation of a ferric-hydroperoxo intermediate (**30**)<sup>28</sup>, which implicates ferric-superoxo as the species that likely abstracts the H-atom from the substrate (**29**→**30**, Fig. 5)<sup>29, 30</sup>. At first glance, the C1-H of (*S*)-2-HPP (**29** in Fig. 5) might seem more activated than the C2-H of (*R*)-**7** (Fig. 4), with the latter bond cleavage requiring the use of a highly reactive iron(IV)-oxo species. However, density functional theory (DFT) calculations indicate that the phosphonate moiety of the substrate provides significant  $\beta$ -stabilization to the C2-centered radical (**14**), such that the bond dissociation energy of the C2-H of (*R*)-1-HPP is actually ~2.7 kcal/mol less than that of the C1-H of (*S*)-2-HPP (93.8 vs. 96.5 kcal/mol)<sup>22</sup>. Thus, a ferric-superoxo species may also be employed by HppE to effect hydrogen atom abstraction from C2 of (*R*)-**7**, allowing the iron(IV)-oxo intermediate generated in a subsequent step to

be utilized for the oxidation of the C2 radical to the cationic intermediate (**14**→**15**, Fig. 4B). In fact, this chemical logic could apply to HppE in reaction with its natural substrate. With a ferric-superoxo intermediate responsible for H-atom abstraction, an iron(IV)-oxo intermediate is available to catalyze the more challenging oxidation of a C1 radical to a carbocation (**31**→**32**, Fig. 5). Indeed, this may be a more common strategy than previously surmised, being utilized by the growing number of identified non-heme iron-dependent enzymes that initiate substrate oxidation using iron-superoxo intermediates<sup>30</sup>. The formation of the iron(IV)-oxo intermediate **31** requires the input of a single electron at the stage of a highly reactive substrate radical intermediate (**30**). The precise timing of this redox reaction may be accomplished by the transfer of an electron from the putative proton-coupled electron transfer pathway of HppE, which is comprised of several tyrosine residues<sup>3</sup>. The resulting protein radical could then be quenched by the external reductant at a subsequent (and not necessarily precisely controlled) time to regenerate the active form of the enzyme. Experiments to further characterize the catalytic mechanism of HppE are in progress.

## Methods Summary

HppE used in this study was purified as described previously<sup>29</sup>. All synthetic and enzymatic reaction products were characterized by NMR spectroscopy and/or high-resolution mass spectrometry. A typical NMR assay contained 0.25 mM HppE, 0.25 mM Fe(NH<sub>4</sub>)<sub>2</sub>(SO<sub>4</sub>)<sub>2</sub>•6H<sub>2</sub>O, 7.5 mM FMN, 25 mM substrate ((*R*)-**7**, (*S*)-**7**, **11**, **12**, (*RR*)-**23**, (*RS*)-**23**, or **27**), and 25 mM NADH in 700 μL of 20 mM Tris buffer (pH 7.5). The conversion of (*RR*)-**23**/*(RS)*-**23** to **26** by HppE was confirmed by spiking the reaction mixture with an authentic standard of **26**. Further details regarding experimental procedures and DFT calculations are described in the Supporting Information.

## Supplementary Material

Refer to Web version on PubMed Central for supplementary material.

## Acknowledgments

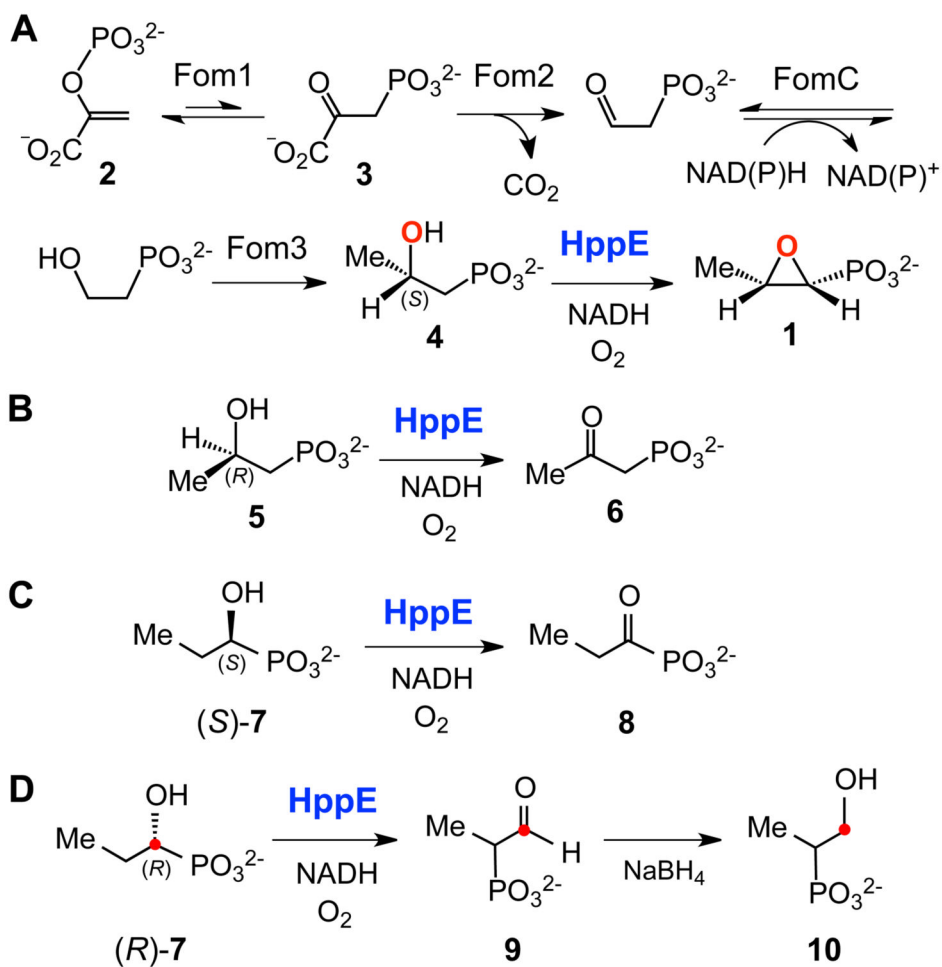
We thank W. Johnson and S. Sorey for assistance with the NMR experiment setup. This work is supported in part by grants from The National Institutes of Health (GM040541 to H.-w.L.) and the Welch Foundation (F-1511). C.L.D. is a Howard Hughes Medical Institute Investigator. The structures of (*R*)- and (*S*)-1-HPP-HppE complex are deposited in the Protein Data Bank with PDB entries 4J1W and 4J1X, respectively. Crystallographic data collection were conducted at the Advanced Light Source, a Department of Energy (DOE) national user facility (Contract DE-AC02-05CH11231), at beamline 8.2.2 operated by the Berkeley Center for Structural Biology, which is supported in part by DOE and NIH/NIGMS.

## References

1. Liu P, et al. Protein purification and function assignment of the epoxidase catalyzing the formation of fosfomycin. *J Am Chem Soc.* 2001; 123:4619–4620. [PubMed: 11457256]
2. Liu P, Liu A, Yan F, Wolfe MD, Lipscomb JD, Liu Hw. Biochemical and spectroscopic studies on (*S*)-2-hydroxypropylphosphonic acid epoxidase: a novel mononuclear non-heme iron enzyme. *Biochemistry.* 2003; 42:11577–11586. [PubMed: 14529267]
3. Higgins LJ, Yan F, Liu P, Liu Hw, Drennan CL. Structural insight into antibiotic fosfomycin biosynthesis by a mononuclear iron enzyme. *Nature.* 2005; 437:838–844. [PubMed: 16015285]

4. Stengel D, et al. Second-line treatment of limb-threatening diabetic foot infections with intravenous fosfomycin. *J Chemother.* 2005; 17:527–535. [PubMed: 16323442]
5. Hammerschmidt F, Bovermann G, Bayer K. Biosynthesis of natural products with a P-C Bond .5. The oxirane oxygen atom of fosfomycin is not derived from atmospheric oxygen. *Liebigs Annalen Der Chemie.* 1990:1055–1061.
6. Marquardt JL, et al. Kinetics, stoichiometry, and identification of the reactive thiolate in the inactivation of UDP-GlcNAc enolpyruvyl transferase by the antibiotic fosfomycin. *Biochemistry.* 1994; 33:10646–10651. [PubMed: 8075065]
7. Brown ED, Vivas EI, Walsh CT, Kolter R. MurA (MurZ), the enzyme that catalyzes the first committed step in peptidoglycan biosynthesis, is essential in *Escherichia coli*. *J Bacteriol.* 1995; 177:4194–4197. [PubMed: 7608103]
8. Ko KS, et al. In vitro activity of fosfomycin against ciprofloxacin-resistant or extended-spectrum beta-lactamase-producing *Escherichia coli* isolated from urine and blood. *Diagn Microbiol Infect Dis.* 2007; 58:111–115. [PubMed: 17300900]
9. Nakazawa H, Kikuchi Y, Honda T, Isago T, Nozaki M. Enhancement of antimicrobial effects of various antibiotics against methicillin-resistant *Staphylococcus aureus* (MRSA) by combination with fosfomycin. *J Infect Chemother.* 2003; 9:304–309. [PubMed: 14691650]
10. Cassone M, Campanile F, Pantosti A, Venditti M, Stefani S. Identification of a variant “Rome clone” of methicillin-resistant *Staphylococcus aureus* with decreased susceptibility to vancomycin, responsible for an outbreak in an intensive care unit. *Microb Drug Resist.* 2004; 10:43–49. [PubMed: 15140393]
11. Seidel HM, Freeman S, Seto H, Knowles JR. Phosphonate biosynthesis: isolation of the enzyme responsible for the formation of a carbon-phosphorus bond. *Nature.* 1988; 335:457–458. [PubMed: 3138545]
12. Liu S, Lu Z, Jia Y, Dunaway-Mariano D, Herzberg O. Dissociative phosphoryl transfer in PEP mutase catalysis: structure of the enzyme/sulfolpyruvate complex and kinetic properties of mutants. *Biochemistry.* 2002; 41:10270–10276. [PubMed: 12162742]
13. Hidaka T, Goda M, Kuzuyama T, Takei N, Hidaka M, Seto H. Cloning and nucleotide sequence of fosfomycin biosynthetic genes of *Streptomyces wedmorensis*. *Mol Gen Genet.* 1995; 249:274–280. [PubMed: 7500951]
14. Woodyer RD, Li GY, Zhao HM, van der Donk WA. New insight into the mechanism of methyl transfer during the biosynthesis of fosfomycin. *Chem Commun.* 2007:359–361.
15. Yan F, Li T, Lipscomb JD, Liu A, Liu Hw. Site-directed mutagenesis and spectroscopic studies of the iron-binding site of (*S*)-2-hydroxypropylphosphonic acid epoxidase. *Arch Biochem Biophys.* 2005; 442:82–91. [PubMed: 16150418]
16. Kovaleva EG, Lipscomb JD. Versatility of biological non-heme Fe(II) centers in oxygen activation reactions. *Nat Chem Biol.* 2008; 4:186–193. [PubMed: 18277980]
17. Zhao Z, Liu P, Murakami K, Kuzuyama T, Seto H, Liu Hw. Mechanistic studies of HPP epoxidase: configuration of the substrate governs its enzymatic fate. *Angew Chem Int Ed Engl.* 2002; 41:4529–4532. [PubMed: 12458528]
18. Yun D, Dey M, Higgins LJ, Yan F, Liu Hw, Drennan CL. Structural basis of regiospecificity of a mononuclear iron enzyme in antibiotic fosfomycin biosynthesis. *J Am Chem Soc.* 2011; 133:11262–11269. [PubMed: 21682308]
19. Yan F, Moon SJ, Liu P, Zhao Z, Lipscomb JD, Liu A, Liu Hw. Determination of the substrate binding mode to the active site iron of (*S*)-2-hydroxypropylphosphonic acid epoxidase using <sup>17</sup>O-enriched substrates and substrate analogues. *Biochemistry.* 2007; 46:12628–12638. [PubMed: 17927218]
20. Costas M, Mehn MP, Jensen MP, Que L Jr. Dioxygen activation at mononuclear nonheme iron active sites: enzymes, models, and intermediates. *Chem Rev.* 2004; 104:939–986. [PubMed: 14871146]
21. Huang H, et al. Evidence for radical-mediated catalysis by HppE: a study using cyclopropyl and methylenecyclopropyl substrate analogues. *J Am Chem Soc.* 2012; 134:13946–13949. [PubMed: 22830643]
22. Details and complete methods are provided in the supplementary information of *Nature* online

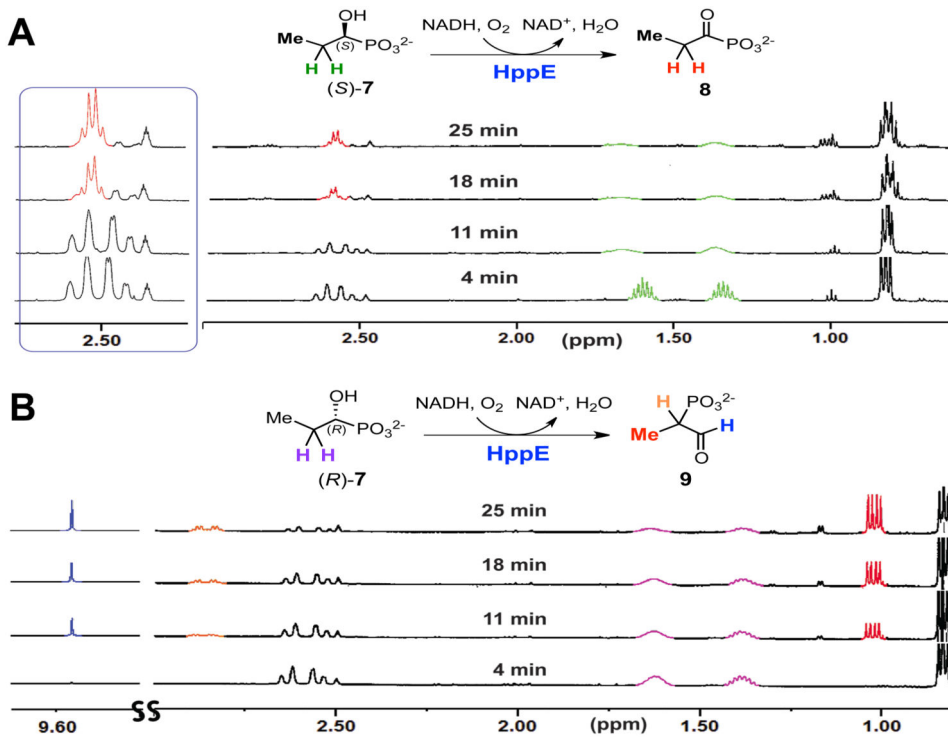
23. Yamashita M, Sugiura M, Oshikawa T, Inokawa S. Synthesis of dimethyl (1-nitromethylalkyl)phosphonates and their conversion to dimethyl (1-formylalkyl)phosphonates by oxidation with ozone. *Synthesis*. 1987; 1:62–64.
24. Churi RH, Griffin CE. 1,2 Shifts of dialkoxyphosphono groups in skeletal rearrangements of alpha,beta-epoxyvinylphosphonates. *J Am Chem Soc*. 1966; 88:1824–1825.
25. Girotra NN, Wendler NL. Synthesis and transformations in the phosphonomycin series. *Tetrahedron Lett*. 1969; 10:4647–4650.
26. Lesburg CA, Caruthers JM, Paschall CM, Christianson DW. Managing and manipulating carbocations in biology: terpenoid cyclase structure and mechanism. *Curr Opin Struct Biol*. 1998; 8:695–703. [PubMed: 9914250]
27. Kappock TJ, Caradonna JP. Pterin-dependent amino acid hydroxylases. *Chem Rev*. 1996; 96:2659–2756. [PubMed: 11848840]
28. Mirica LM, McCusker KP, Munos JW, Liu Hw, Klinman JP. <sup>18</sup>O kinetic isotope effects in non-heme iron enzymes: probing the nature of Fe/O<sub>2</sub> intermediates. *J Am Chem Soc*. 2008; 130:8122–8123. [PubMed: 18540575]
29. Yan F, Munos JW, Liu P, Liu Hw. Biosynthesis of fosfomycin, re-examination and re-confirmation of a unique Fe(II)- and NAD(P)H-dependent epoxidation reaction. *Biochemistry*. 2006; 45:11473–11481. [PubMed: 16981707]
30. van der Donk WA, Krebs C, Bollinger JM. Substrate activation by iron superoxo intermediates. *Curr Opin Struct Biol*. 2010; 20:673–683.

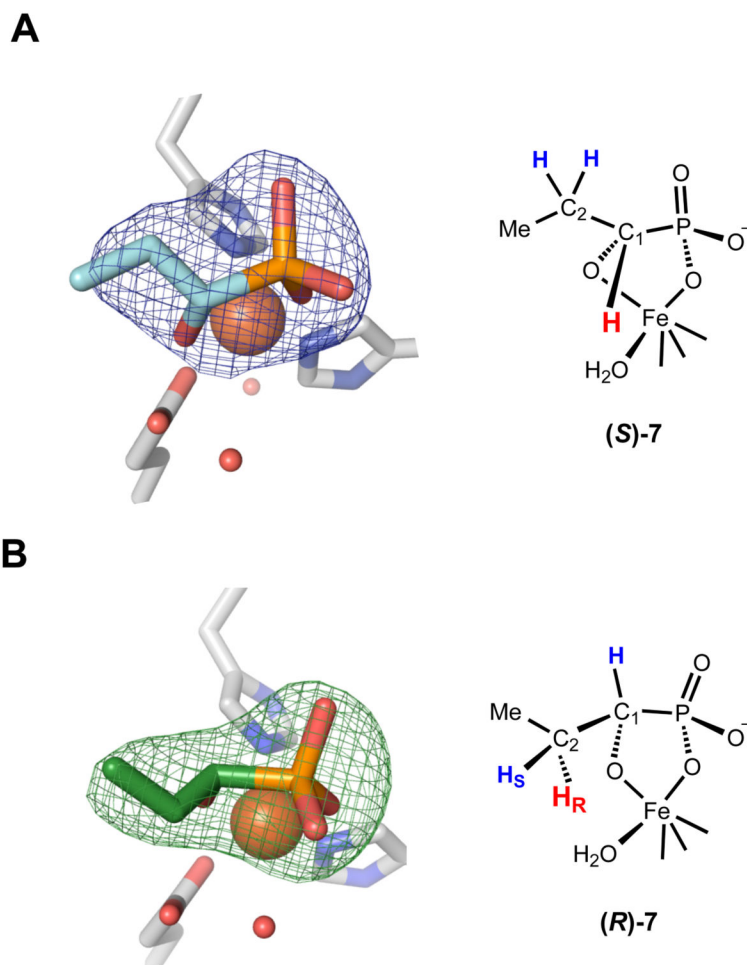


**Figure 1. Fosfomycin biosynthetic pathway and HppE-catalyzed conversion of various substrate analogues**

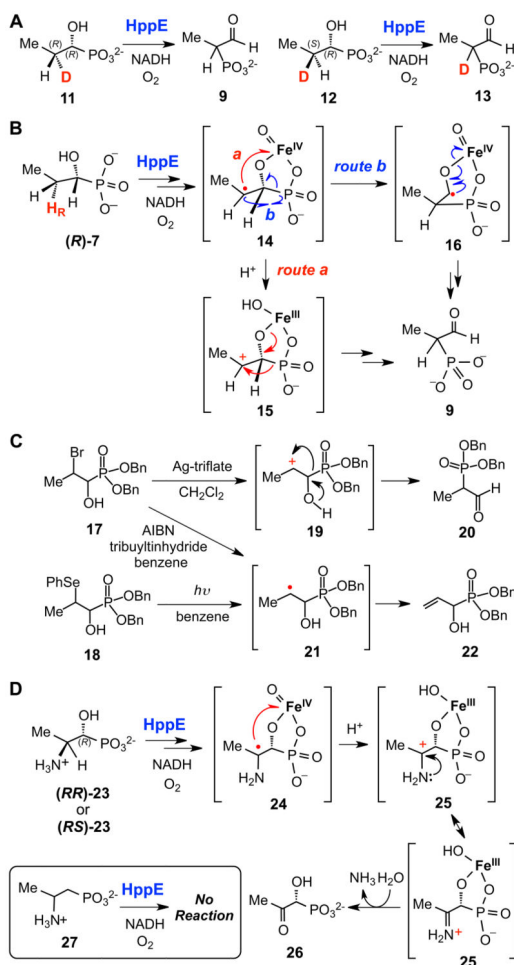
(A) Formation of fosfomycin (1) from PEP (2). (B) Conversion of (*R*)-2-HPP (5) to the corresponding ketone 6. (C) Conversion of (*S*)-1-HPP to acyl phosphonate (8). (D) Conversion of (*R*)-1-HPP (7) to the aldehyde product (9).







**Figure 3. Structures of (S)-7 and (R)-7 bound to the iron center of HppE in a bidentate mode** (A) (S)-7 (carbons in blue) in  $F_o-F_c$  omit map density contoured at  $6\sigma$  (left) and its chemical structure (right), with hydrogen atoms accessible for abstraction in red and inaccessible in blue. The putative dioxygen binding site on Fe is partially occupied by water molecules (red spheres) in both of these structures (Fe-H<sub>2</sub>O distances are 3.7 and 3.0 Å). Colors: Fe in rust, P in orange, O in red, N in blue, protein C in gray. (B) (R)-7 (carbons in green) in  $F_o-F_c$  omit map density contoured at  $6\sigma$  (left) and its chemical structure (right). Hydrogen atoms labeled as in (A).

**Figure 4.**

(A) Stereochemistry of hydrogen atom abstraction from (*R*)-1-HPP (**7**) determined using the stereospecifically deuterated compounds **11** and **12**. (B) Hypothetical mechanisms for HppE-catalyzed 1,2-phosphono migration involving cation (route a) and radical (route b) mediated rearrangements. Intermediate **14** could be generated in a manner analogous to the formation of **31** from (*S*)-2-HPP (see Fig. 5). (C) Model reactions to probe the involvement of radical or cation intermediates in the 1,2-phosphono migration catalyzed by HppE. The migration product is only observed when cation **19** is formed from **17** using silver-triflate. (D) HppE-catalyzed conversion of (*RR*)- and (*RS*)-**23** to the imine hydrolysis product **26**, consistent with the oxidation of (*R*)-**7** to a cationic intermediate by a reactive iron-oxygen species. Inset: Compound **27**, which lacks the C1 hydroxyl group, is not a substrate of HppE, indicating that the amino group is not capable of supporting the bidentate substrate coordination required for catalysis.

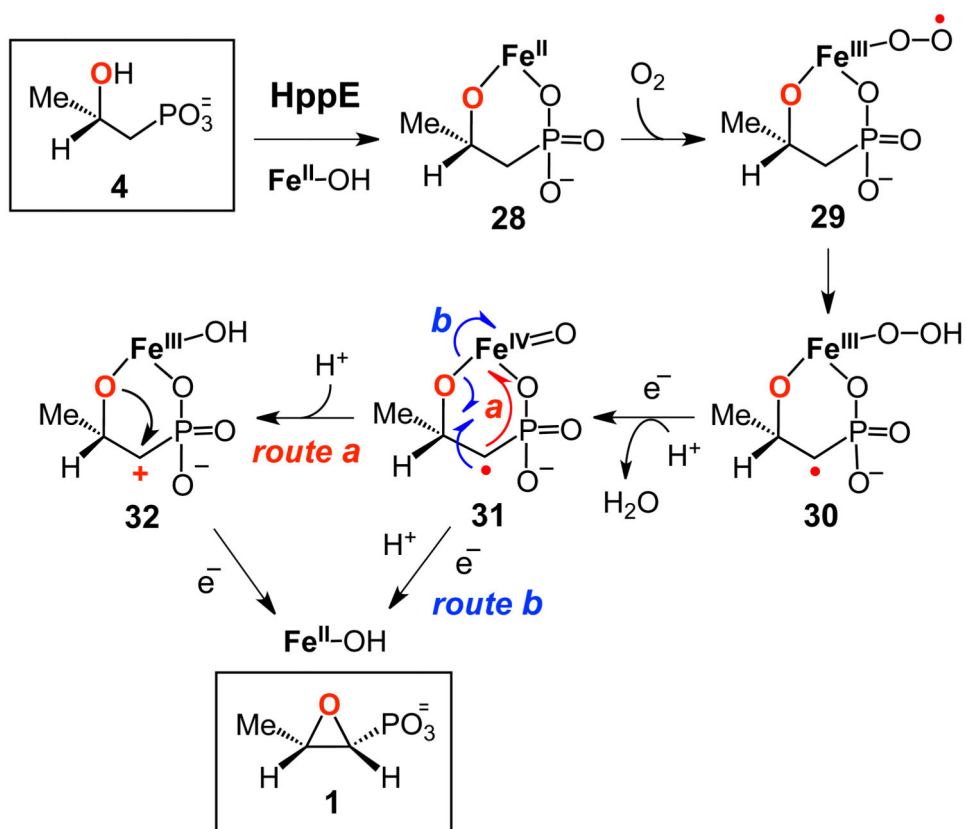


**Figure 5.** Revised mechanisms for the HppE-catalyzed epoxidation of (S)-2-HPP (4) involving C1 cation formation (route a) or O-atom rebound (route b).